Interner Bericht
DESY F41-69/6
Oktober 1969

Optical Transitions from Inner Shells in Solid Rare Gases

R. Haensel, G. Keitel, C. Kunz, P. Schreiber and B. Sonntag

II. Institut für Experimentalphysik der Universität Hamburg,
Hamburg, Germany

and

Deutsches Elektronen-Synchrotron, Hamburg, Germany

Paper given at the X. European Congress for Molecular Spectroscopy,
Sept. 29 - Oct. 3, 1969, Liege, Belgien

Optical Transitions from Inner Shells in Solid Rare Gases

R. Haensel, G. Keitel, C. Kunz, P. Schreiber and B. Sonntag

II. Institut für Experimentalphysik der Universität Hamburg, Hamburg, Germany

and

Deutsches Elektronen-Synchrotron, Hamburg, Germany

I. Introduction

In the preceding paper F.C. Brown[1] has outlined the previous lack of radiation sources for photon energies above 20 eV and the fact that synchrotron radiation has now become a powerful source for covering this formerly inaccessible energy range. With this new source measurements of optical excitations from inner shells are now possible for many materials. The use of synchrotron radiation is also interesting for valence band transitions for wide band gap materials such as alkali halides and solid rare gases because they only begin to absorb in the range of 5 to 15 eV and characteristic features in the valence band absorption extend to the spectral range above 20 eV.

In the last few years a number of optical measurements have been performed at the Deutsches Elektronen-Synchrotron DESY, a 7.5 GeV electron synchrotron, on light metals[2-5], transition metals[6] and

heavy metals[7-9], as well as on semiconductors[10], alkali halides[11-14] and solid rare gases[15-17]. Since the preceding paper[1] concentrated on measurements on alkali halides, we will review our solid rare gas results.

The solid rare gases Ne, Ar, Kr and Xe are formed from atoms whose outer shells are filled with electrons with p symmetric wave functions. The electrons of the filled outer shell have large binding energies. Figure 1 gives the thresholds for transitions in the case of free atoms from different shells in the investigated energy region.

Baldini[18] has studied the optical properties of the solid rare gases up to 14 eV, but apart from the Ar K-absorption[19] no excitation of inner shells have been measured in solid rare gases.

Three aspects of inner shell absorption features will be discussed in chapter III after a short description of the experimental arrangement:

a) Optical excitations from inner shells allow for studying final states which optically cannot be reached from the p symmetric valence band. Therefore, the fine structure gives additional information on the final states near the threshold.

b) The measurement of the continuum absorption far from the threshold, especially of d symmetric initial states, shows characteristic shapes due to the atomic potential which differs from the hydrogenic Coulomb potential.

c) Characteristic absorption line shapes have been found; these are due to the interaction between discrete and continuum final states.

II. Experimental Details

The general characteristics of synchrotron radiation[20] and particularily that at DESY[21] are described elsewhere. Therefore, Fig. 2 only demonstrates the spectral distribution. The most characteristic difference as compared to the Stoughton electron storage ring[1] is that the spectral distribution extends to the X-ray region (0.1Å). The background caused by the high energy part of the synchrotron radiation is suppressed by the premirror M (Fig. 3). The Rowland-spectrometer used in the experiments was a 1 m grazing incidence instrument having a 2400 lines/mm grating with a wavelength resolution of about 0.1 Å. The samples were prepared by evaporation onto carbon foils as thin films having a thickness of several hundred Å. The substrates were cooled in a cryostat mounted in front of the entrance slit and the premirror. The best data were obtained when the samples were prepared at a temperature slightly below the sublimation temperature (at 10^{-6} Torr), i. e. 55° K for Xe, 40° K for Kr, 20° K for Ar and 8° K for Ne.

III. Results and Discussion

Continuum Absorption

According to a hydrogen-like model the absorption cross section of free atoms will increase stepwise when the photon energy exceeds the threshold for ionization of an inner shell and will decrease monotonically starting from the threshold as the photon energy increases. This model, which holds in the X-ray region, breaks down in the vacuum-uv. One reason for this is that the average electric field due to nuclear and electronic charges differs from the Coulomb law in the outer region of the atom from which the electrons contributing to the absorption in the

vacuum-uv mainly stem. In this region of the atom the attractive electric force is balanced by the centrifugal repulsion. The resulting force can be attractive or repulsive depending on the atomic number Z and on the radial quantum number l.

Repulsive centifugal barriers which show up especially for high radial quantum numbers l have a strong effect on the absorption. They suppress the overlapping of initial and final state wave functions at the threshold and thereby reduce the optical absorption at the threshold and shift the bulk of the absorption to higher energies. This phenomenon has been quantitatively worked out by Manson and Cooper[22], McGuire[23] and Combet Farnoux[24].

These theories are atomic theories and, therefore, do not include solid state effects such as crystal fields etc. On the other hand one should expect that far from the threshold the absorption of solids should not be too different from the absorption of free atoms, since the wave functions forming the conduction band adopt more and more plane wave like character.

The shift of oscillator strengths to higher energies has been observed in Xe[25] gas, where the effect was seen for the first time, later also in metals[7-9] and in the alkali halides[1,26]. We found it especially interesting to compare the absorption behaviour of one material in the atomic and in the solid state. Figure 4 shows the absorption curve of gaseous and solid Xe in the energy range 60 to 140 eV. The gas absorption cross section is in excellent agreement with Ederer's[25]

results, the solid curve has been normalized by setting the integrated oscillator strength over the entire energy range equal for both states, as no thickness determinations of the solid Xe films have been made.

At about 65 eV we see the onset of transitions from the 4d shell; the fine structure in the vicinity of the threshold will be discussed later. Near 80 eV, where Codling and Madden[27] have detected multiple excitations of 4d and 5p electrons in the gas, we also see some fine structure in the solid which is probably due to a double excitation. This is very interesting in view of contradictory theoretical predictions by Miyakawa[28] and Hermanson[29] on the relative oscillator strength of single and multiple excitations in wide band gap materials. Our results favour more Hermanson's[29] theory which predicts that for multiple excitation the oscillator strength is 1 to 2 orders of magnitude smaller than that of single excitations.

It is remarkable that after the normalization of the integrated oscillator strength there is excellent agreement of both curves before the onset of the 4d transitions and also over the entire range of the d→f bulk absorption peak. Near 140 eV we see absorption structures due to 4d transitions. An interesting fact is that in the gas only transition from the 4p (3/2) shell can be seen. Near 152 eV, where transitions from the 4p (1/2) shell are expected, no structure has been found in the gas. This fact has been explained by Codling and Madden[30] as being caused by the interaction between the 4p (1/2) discrete final states and the 4p (3/2) continuum. In contrast to the gas in solid Xe some structure near 150 eV can be seen.

In Kr (Fig. 5) the onset of 3d transitions is at about 90 eV. At 127 eV, the upper limit in our present experiment, the maximum of the d→f transitions is almost reached. That means that the continuum absorption cross section is in the same order as in the d→p transition lines in contrast to the behaviour of the cross section in Xe. In Xe the d→f maximum is much stronger than the lines. Fano and Cooper[31] explain the strong maximum at 100 eV in Xe as being a "resonance near threshold" because 4d→4f transitions are possible within the same main shell which, however, are not possible for the Kr 3d transitions. Normalization on the integrated oscillator strength once more leads to excellent agreement for the absorption coefficient before the 3d onset as well as in the continuum absorption range.

According to Madden and Codling[27] the fine structure in the gas around 110 eV is again due to double excitation (3d + 4p), but no obviously corresponding structure can be seen in the solid at this photon energy.

Absorption Fine Structure

In Fig. 6 we see close to 90 eV the onset of 3d transitions in Kr on an enlarged scale. As a comparison the gas lines have also been measured and their positions serve as energy calibration marks[32]. The specific 3d structure is situated on a residual continuum absorption brought about by transitions from outer shells to high lying states of the conduction band or ionization continuum resp. The first peak A at 90.28 eV is followed by many other absorption structures. The most prominent structures can be ordered in pairs. They are labeled with unprimed and primed capital letters. All pairs have an energy distance of about 1.2 eV, the spin orbit splitting energy of the 3d shell in Kr[32]. Very similar features can be seen in the 4d transitions of Xe (Fig. 7).

As the initial state has d symmetry and the lowest point of the conduction band at Γ_1 has s symmetry in Kr[33] as well as in Xe[34], interband transitions as well as "allowed" exciton series[35] to the lowest point of the conduction band should be optically forbidden. However, according to Elliot[35], "forbidden" exciton series which have all Rydberg-members except $n = 1$ may couple to the Γ_1 point.

The half width of the Kr 3d absorption peaks of $\sim$ 0.15 eV is broader than that of the first excitonic transitions in the fundamental absorption region[18]. Therefore, they could possibly be attributed to interband transitions rather than to excitonic ones. However, the line width of the first 3d peaks is the same as for the gas peaks and, therefore, may be explained as due to lifetime broadening of the 3d initial state as was the case for the gas[30]. Furthermore, our energy distribution measurements of photoelectrons in NaCl[13] have favoured the existence of core excitons which may also exist for the d transitions of Kr and Xe.

Assuming the first peaks to be excitons the B,B' and C,C' in solid Kr (Fig. 6) may be understood as the $n = 2$ and $n = 3$ members of a forbidden exciton series. The peak A then has approximately the energy position to be explained as a rudiment of the $n = 1$ exciton. The series' limit at 92.3 eV would, as compared with the band gap for valence band transitions of 11.67 eV[18], give a difference between the valence band and the 3d shell of 80.6 eV. This is almost the value for the gas (79.8 eV) which is derived from the gas ionization limits for 4p transitions (14.00 eV[36]) and 3d transitions (93.82 eV[32]). The corresponding interpretation for Xe leads to a similar difference between the 5p and 4d shells binding energies in solid and atomic Xe.

Another possible explanation is to assume that B and C are not members of a Rydberg-series, but that they are $n = 1$ excitons to different p or f symmetric points in the conduction band. Those points, however, appear only several eV above the bottom of the conduction band[33,34], thus causing the excitons to have binding energies of ~ 5 eV.

As no theoretical calculations are as yet available for the properties of core excitons a definitive decision for one of the 2 possibilities of interpretation is difficult.

Line Shape

The profiles of the absorption structure considered so far are Lorentzian shaped absorption lines situated on a continuum absorption background.

In many cases of atomic rare gas absorption Madden and Codling[30] have also detected other types of absorption profiles such as asymmetric profiles and "window" lines. These line profiles are due to the interaction of the discrete states with the underlying continuum. Fano and Cooper[37] have developed a general theory on the line profiles. They derived a formula for the description of the profiles

$$\sigma(E) = \sigma_a \frac{(q+\varepsilon)^2}{1+\varepsilon^2} + \sigma_b$$

where σ is the total absorption cross section at the energy E, σ_a the interacting, σ_b the non interacting part, q is an interaction index. Assuming a constant ratio σ_a/σ_b the value of q is small for window, intermediate for asymmetric and large for enhanced absorption profiles. ε is the energy difference to the resonance energy

E_r in units of the line width Γ as:

$$\varepsilon = \frac{E - E_r}{\frac{1}{2}\Gamma}$$

We were interested in studying whether the window profiles of the Ar 3s transitions[38] and the asymmetric profiles of the Ne 2s transitions[39] are preserved in the solids. We have measured the absorption of solid Ar (Fig. 8) and of solid and gaseous Ne (Fig. 9). The structures are broadened; but the main character is clearly preserved in both cases.

References

1) F.C. Brown, C. Gähwiller, H. Fujita, N. Carrera and W. Scheifley, preceding paper

2) R. Haensel, B. Sonntag, C. Kunz and T. Sasaki, J. Appl. Phys. 40, 3046 (1969)

3) R. Haensel, G. Keitel, P. Schreiber, B. Sonntag and C. Kunz, Phys. Rev. Letters 23, 528 (1969)

4) M. Skibowski, B. Feuerbacher, W. Steinmann and R.P. Godwin, Z. Physik 211, 329 + 342 (1968)

5) B.P. Feuerbacher, R. P. Godwin and M. Skibowski, Z. Physik 224, 172 (1969)

6) B. Sonntag, R. Haensel and C. Kunz, Sol. State Comm. 7, 597 (1969)

7) R. Haensel, C. Kunz and B. Sonntag, Phys. Letters 25A, 205 (1967)

8) R. Haensel, C. Kunz, T. Sasaki and B. Sonntag, Appl. Opt. 7, 301 (1968)

9) R. Haensel, K. Radler, B. Sonntag and C. Kunz, Sol. State Comm., 7, 1495 (1969)

10) B. Feuerbacher, M. Skibowski, R.P. Godwin and T. Sasaki, J. Opt. Soc. Am. 58, 1434 (1968)

11) R. Haensel, C. Kunz and B. Sonntag, Phys. Rev. Letters 20, 262 (1968)

12) R. Haensel, C. Kunz, T. Sasaki and B. Sonntag, Phys. Rev. Letters 20, 1436 (1968)

13) R. Haensel, G. Keitel, G. Peters, P. Schreiber, B. Sonntag and C. Kunz, Phys. Rev. Letters 23, 530 (1969)

14) D. Blechschmidt, R. Klucker and M. Skibowski, Phys. Stat. Sol. (in press), preprint DESY 69/27

15) R. Haensel, G. Keitel, P. Schreiber and C. Kunz, Phys. Rev. Letters 22, 398 (1969)

16) R. Haensel, G. Keitel, P. Schreiber and C. Kunz, Phys. Rev. (in press), preprint DESY 69/23

17) R. Haensel, G. Keitel, C. Kunz and P. Schreiber, to be published

18) G. Baldini, Phys. Rev. 128, 1562 (1962)

19) J.A. Sooles and C.H. Shaw, Phys. Rev. 113, 470 (1959)

20) R.P. Godwin, in Springer Tracts in Modern Physics, Vol. 51, ed. G. Höhler (Springer Verlag, Berlin, Heidelberg, New York 1969)

21) R. Haensel and C. Kunz, Z. Angew. Phys. 23, 276 (1967)

22) S.T. Manson and J.W. Cooper, Phys. Rev. 165, 126 (1968)

23) E.J. McGuire, Phys. Rev. 175, 20 (1968)

24) F. Combet Farnoux, J. Physique 30, 521 (1969)

25) D.L. Ederer, Phys. Rev. Letters 13, 760 (1964)

26) H. Fujita, C. Gähwiller and F.C. Brown, Phys. Rev. Letters 22, 1369 (1969)

27) K. Codling and R.P. Madden, Appl. Opt. 4, 1431 (1965)

28) T. Miyakawa, J. Phys. Soc. Japan 17, 1898 (1962)

29) J.C. Hermanson, Phys. Rev. 177, 1234 (1969)

30) R.P. Madden and K. Codling, in Autoionization, Astrophysical, Theoretical and Laboratory Experimental Aspects, ed. by A. Tempkin (Mono Book Corporation, Baltimore, Md, 1966) p 129

31) U. Fano and J.W. Cooper, Rev. Mod. Physics 40, 441 (1968)

32) K. Codling and R.P. Madden, Phys. Rev. Letters 12, 106 (1964)

33) W.B. Fowler, Phys. Rev. 132, 1591 (1963)

34) M.H. Reilly, J. Phys. Chem. Solids 28, 2067 (1967)

35) R.J. Elliot, Phys. Rev. 108, 1384 (1957)

36) Ch. Moore, NBS Circular 467, Vol. I (1949)

37) U. Fano and J.W. Cooper, Phys. Rev. 137, A 1364 (1964)

38) R.P. Madden, D.L. Ederer and K. Codling, Phys. Rev. 177, 136 (1969)

39) K. Codling, R.P. Madden and D.L. Ederer, Phys. Rev. 155, 26 (1967)

Figure Captions

Fig. 1 Energy thresholds for transitions in free atoms from the inner shells of Ne, Ar, Kr and Xe.

Fig. 2 Spectral distribution of the synchrotron radiation emitted by single electrons of different energies at DESY.

Fig. 3 Experimental arrangement for the solid rare gas thin film absorption measurements. EO = electron orbit, V = valve, Sh = shielding, BS = beam shutter, CW = chopper wheel, Mo = monitor (Cu-Be sheet), F = filter, C = Cryostat, M = mirror, ES = entrance slit of the Rowland monochromator, RA = rotating arm, G = grating, D = detector (photomultiplier behind the exit slit).

Fig. 4 Cross section versus photon energy for solid (solid curve) and gaseous (dashed curve) xenon in the energy range 64 - 155 eV. The inset shows the cross sections in the region of 4p electron excitation in an extended scale.

Fig. 5 Cross section versus photon energy for solid (solid curve) and gaseous (dashed curve) krypton in the energy range 90 - 128 eV.

Fig. 6 Cross section versus photon energy for solid (solid curve) and gaseous (dashed curve) krypton near the onset of 3d electron excitation. The cross section for the solid has been multiplied by a factor of two.

Fig. 7 Cross section versus photon energy for solid (solid curve) and gaseous (dashed curve) xenon near the onset of 4d electron excitation. The cross section for the solid has been multiplied by a factor of two.

Fig. 8 Absorption spectrum of solid Ar (solid curve) at the onset of 3d transitions. For comparison the absorption spectrum of atomic Ar (dashed curve) has been taken from Madden, Ederer and Codling[38].

Fig. 9 Absorption spectrum of solid (solid curve) and atomic (dashed curve) Ne near the onset of 2s transitions.

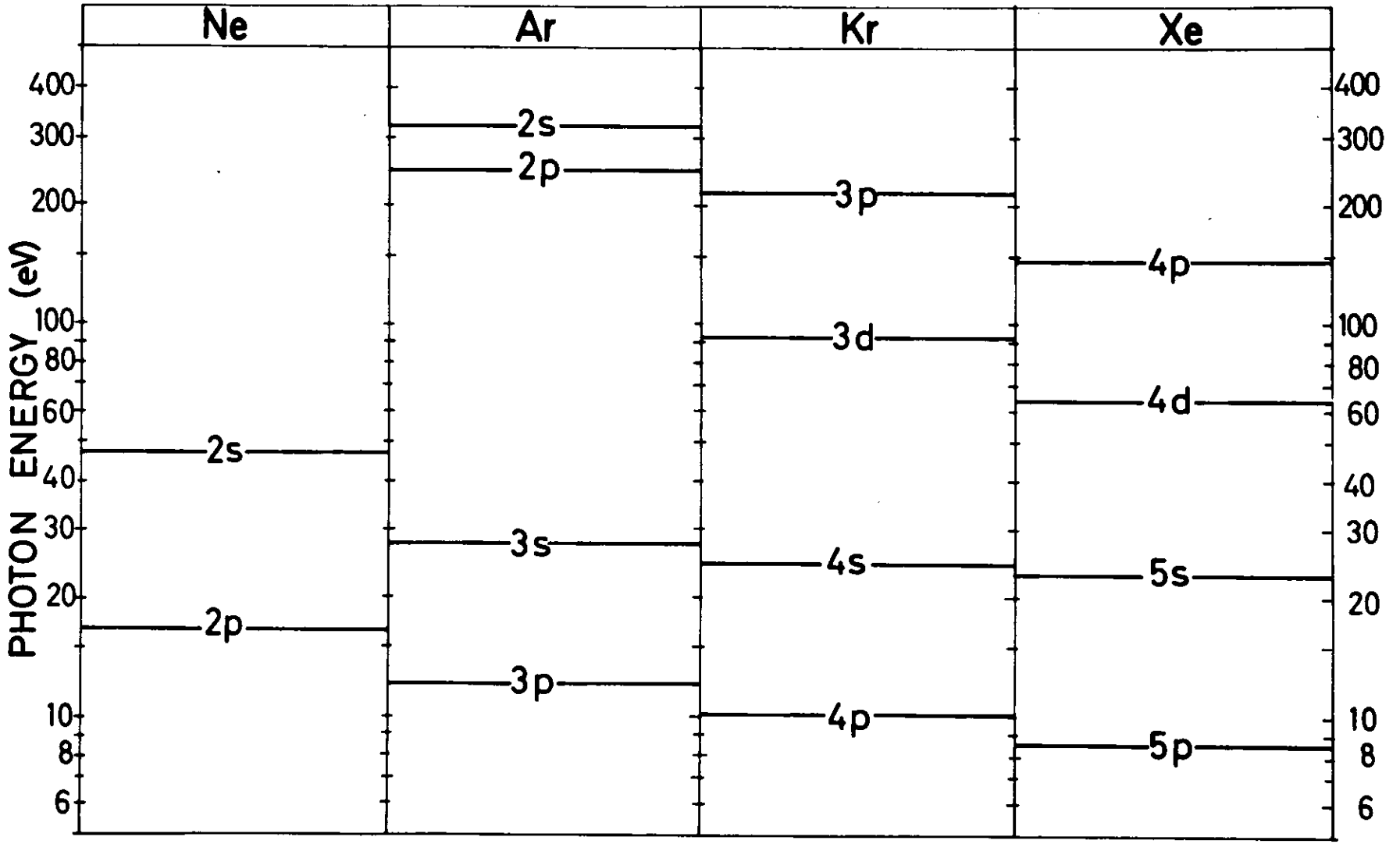
Ne
Ar
Kr
Xe
PHOTON ENERGY (eV)
400
300
200
100
80
60
40
30
20
10
8
6
2s
2p
3s
3p
3d
4s
4p
4d
5s
5p

Fig.1

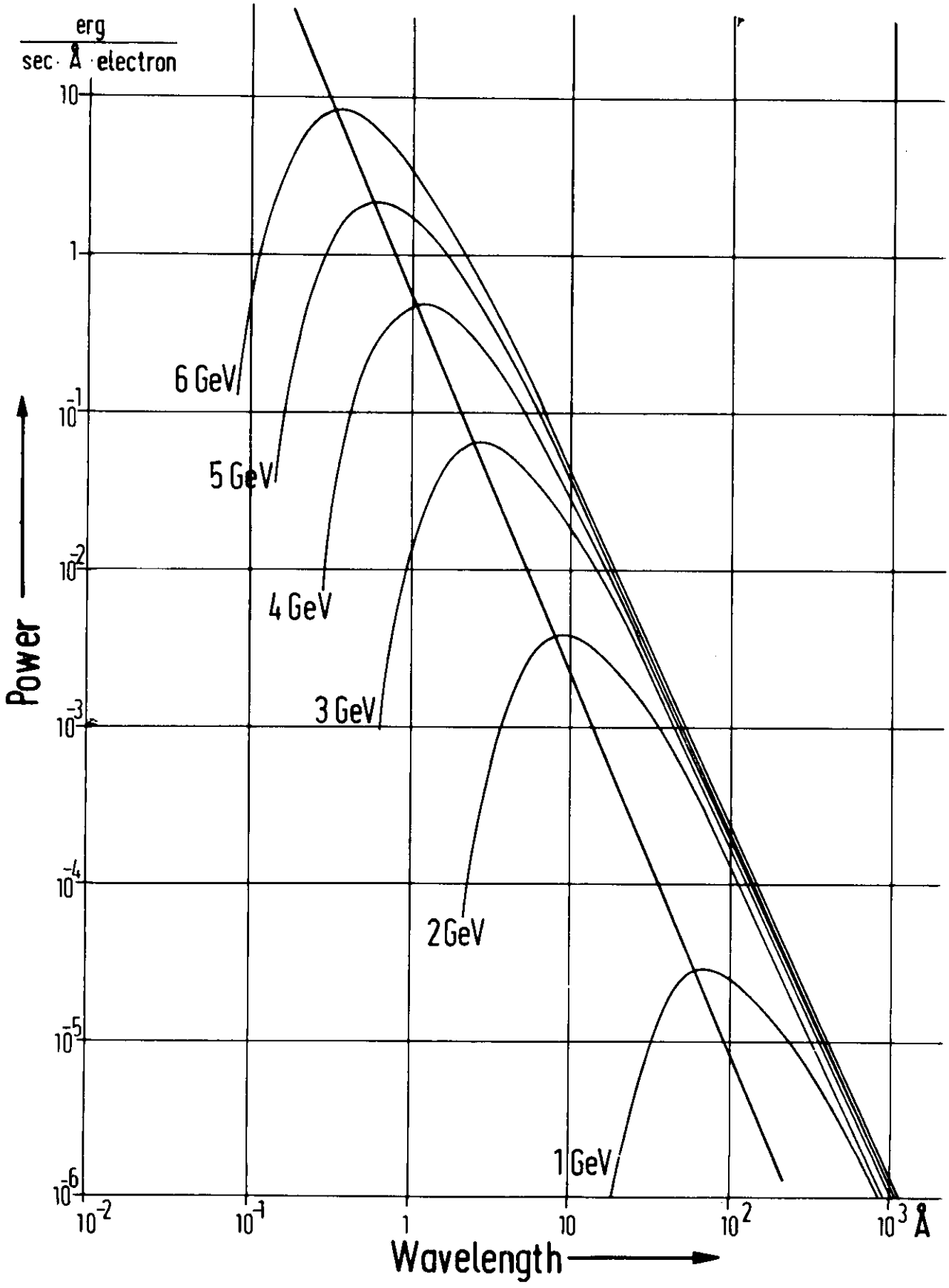
erg
sec · Å · electron
10
1
10^{-1}
10^{-2}
10^{-3}
10^{-4}
10^{-5}
10^{-6}
Power
6 GeV
5 GeV
4 GeV
3 GeV
2 GeV
1 GeV
10^{-2}
10^{-1}
1
10
10^{2}
10^{3} Å
Wavelength

Fig. 2

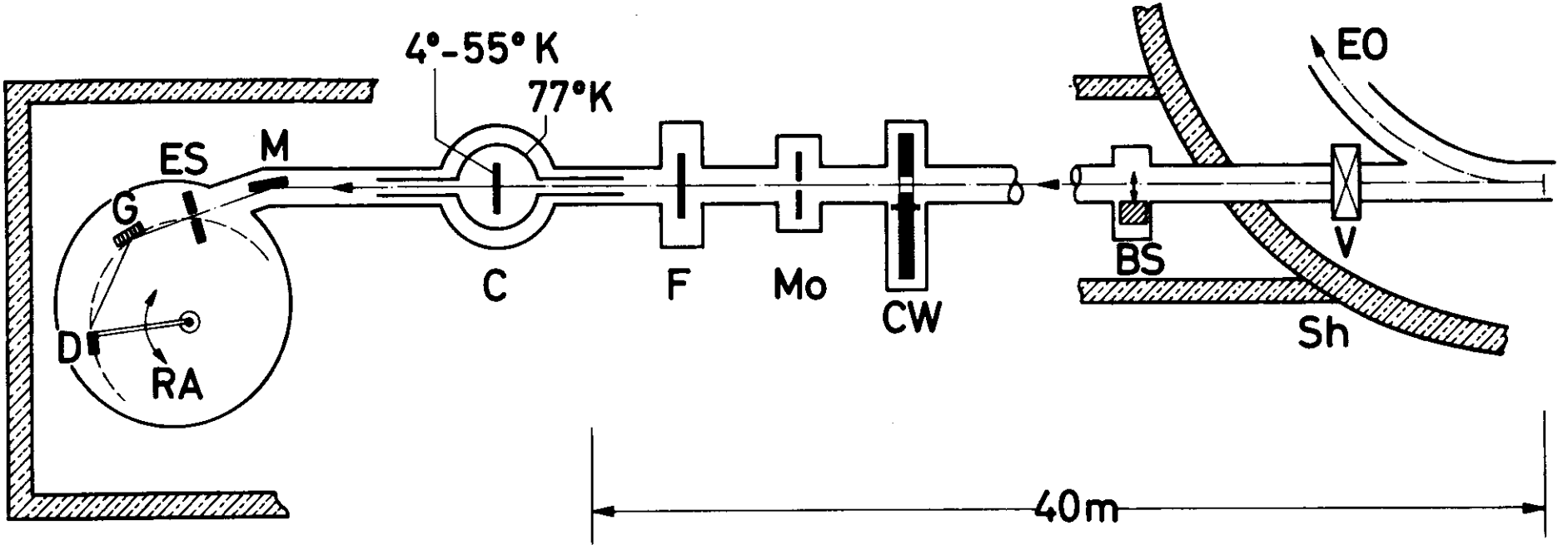

Fig. 3

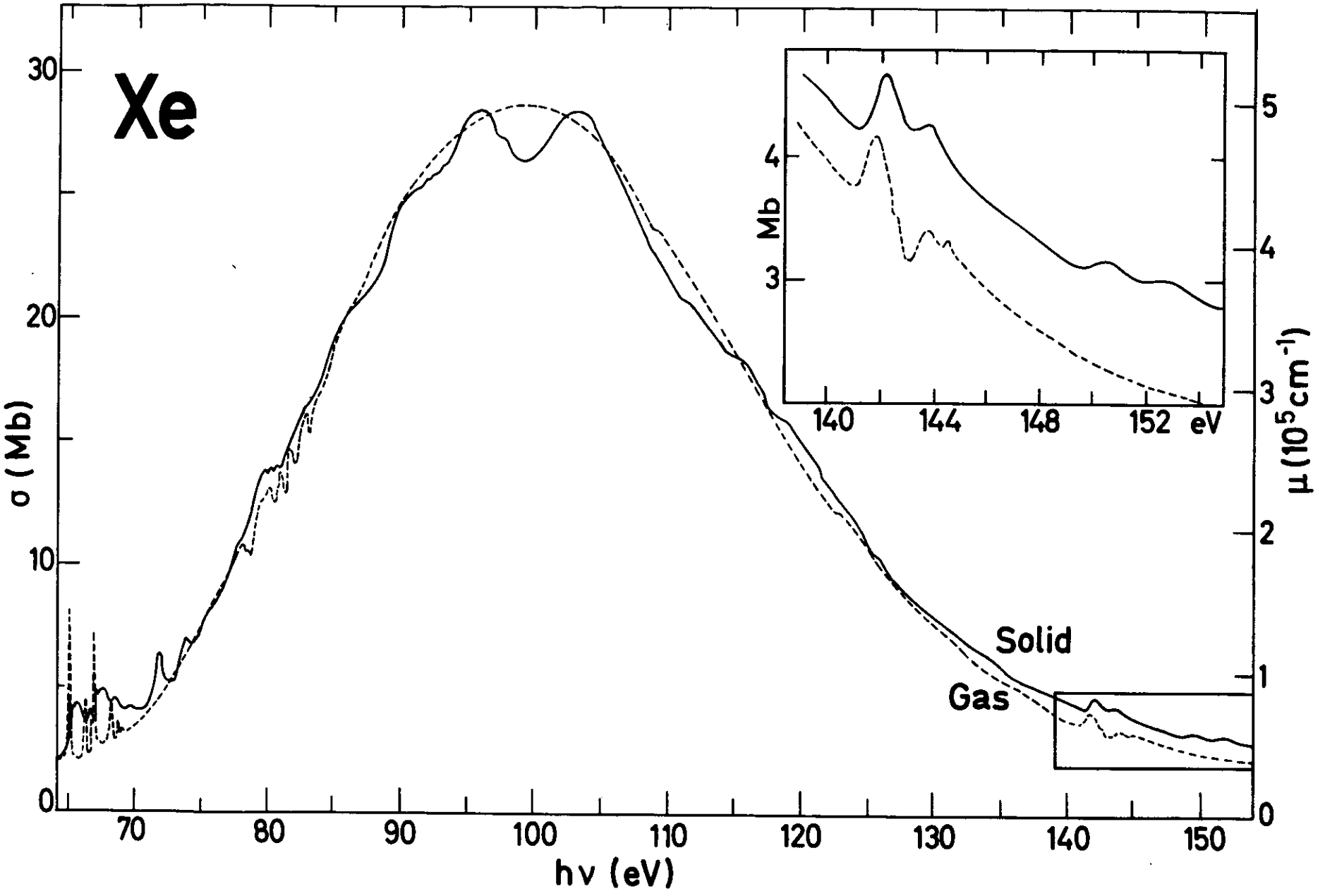
Xe
σ (Mb)
μ (10⁵cm⁻¹)
hν (eV)
Solid
Gas
Mb
eV
0
10
20
30
70
80
90
100
110
120
130
140
150
3
4
5
140
144
148
152

Fig.4

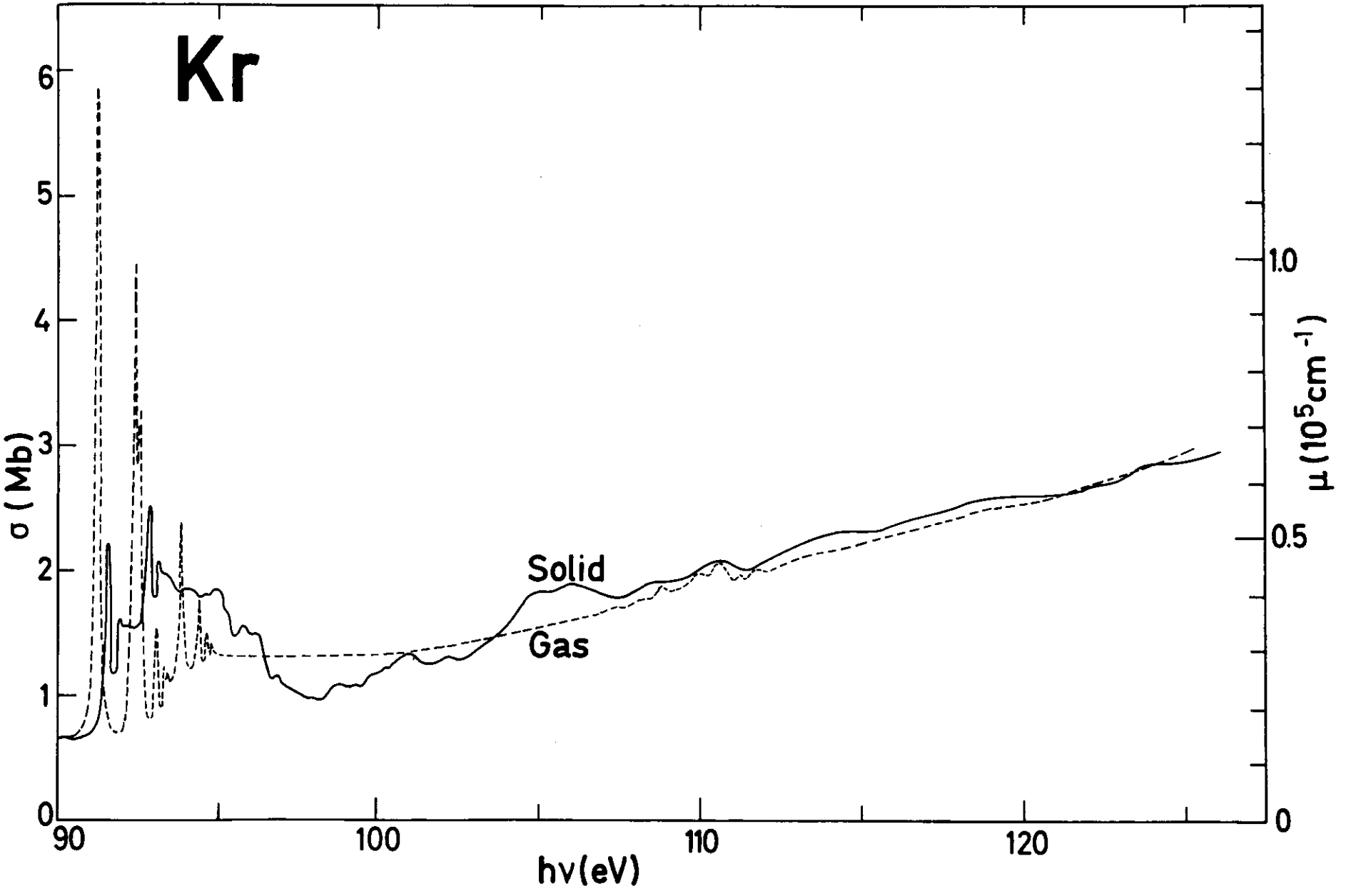

Fig.5

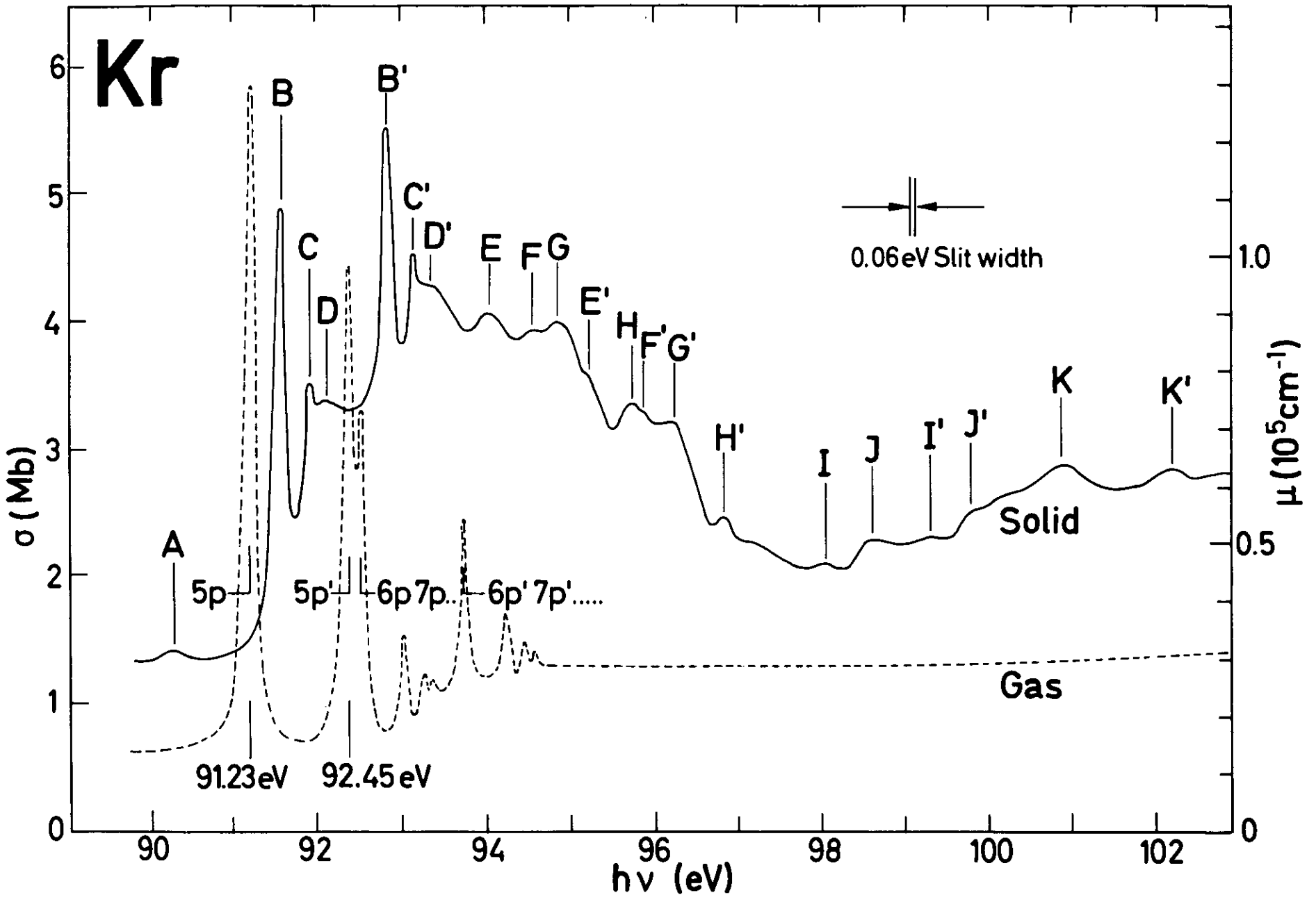
Kr
A
B
B'
C
C'
D
D'
E
F
G
E'
H
F'
G'
H'
I
J
I'
J'
K
K'
5p
5p'
6p 7p..
6p' 7p'.....
0.06eV Slit width
Solid
Gas
91.23eV
92.45eV
σ (Mb)
μ (10^5cm^-1)
hν (eV)
0
1
2
3
4
5
6
90
92
94
96
98
100
102
0
0.5
1.0

Fig.6

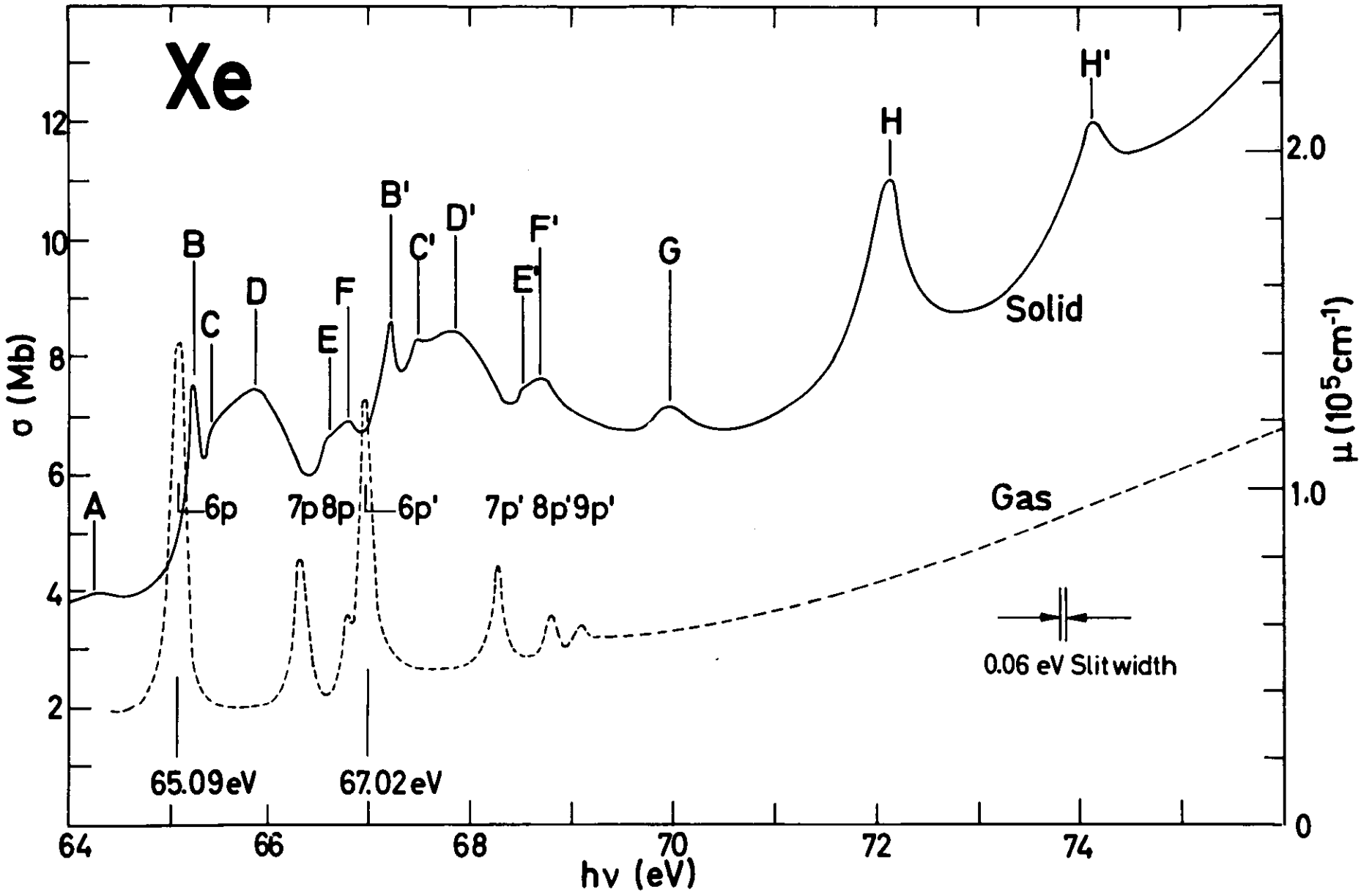
Xe
σ (Mb)
μ (10^5 cm^-1)
hν (eV)
A
B
C
D
E
F
B'
C'
D'
E'
F'
G
H
H'
6p
7p 8p
6p'
7p' 8p' 9p'
Solid
Gas
0.06 eV Slit width
65.09 eV
67.02 eV

Fig. 7

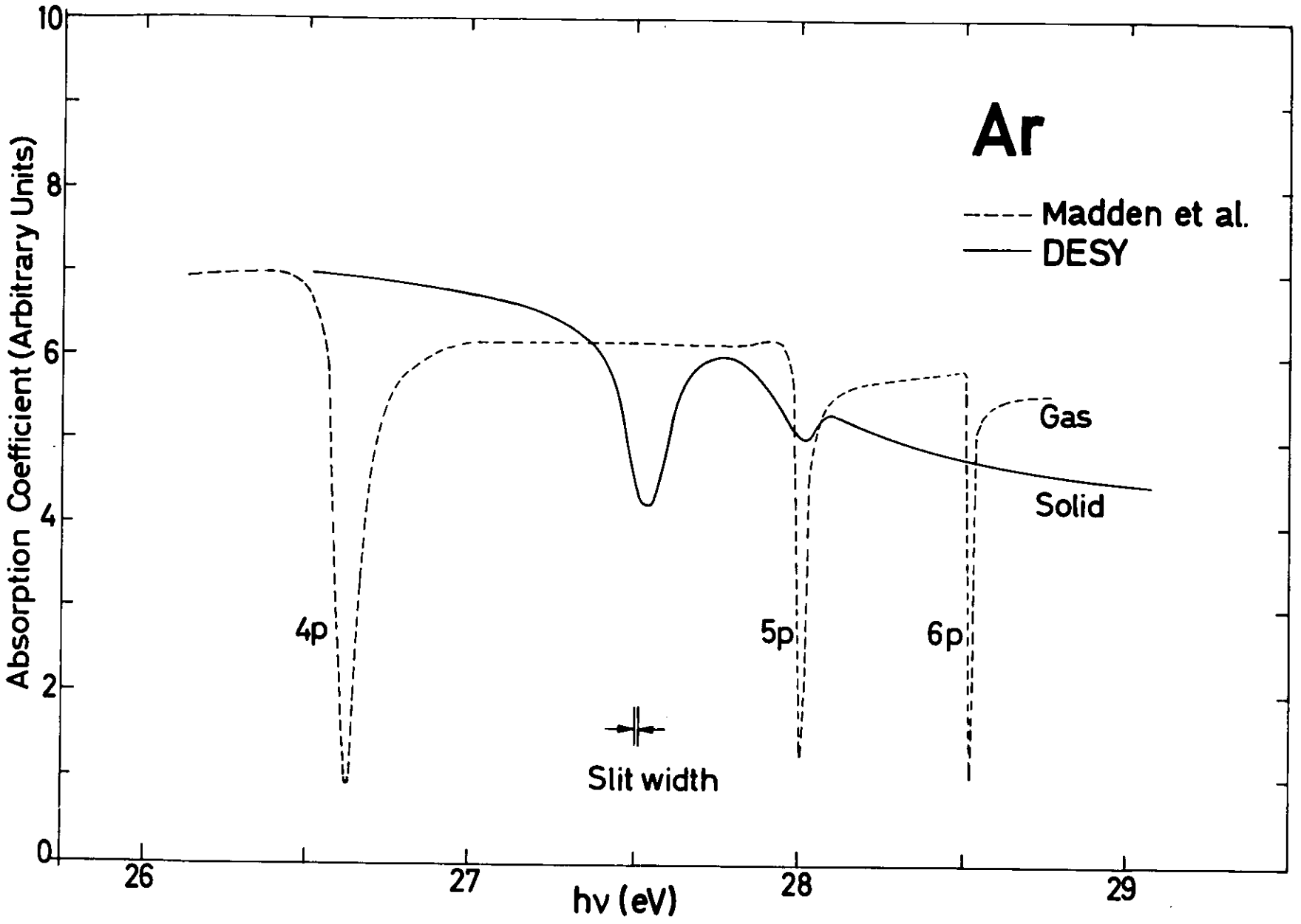
Ar
Madden et al.
DESY
Gas
Solid
4p
5p
6p
Slit width
Absorption Coefficient (Arbitrary Units)
hν (eV)
0
2
4
6
8
10
26
27
28
29

Fig. 8

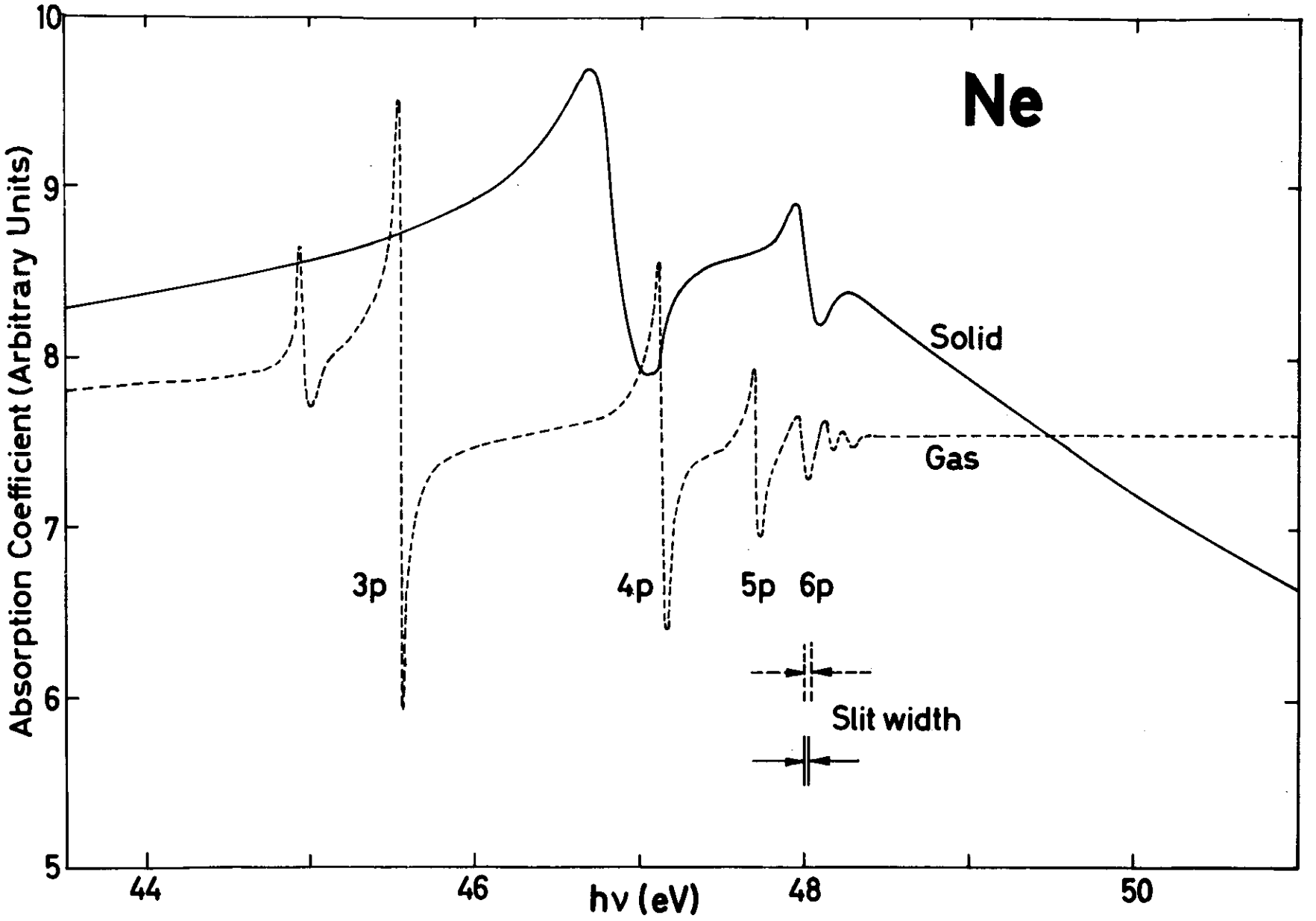
Ne
Absorption Coefficient (Arbitrary Units)
10
9
8
7
6
5
44
46
48
50
hν (eV)
Solid
Gas
3p
4p
5p
6p
Slit width

Fig.9